Catalytic pyrolysis of recalcitrant, insoluble humin byproducts from C6 sugar biorefineries

Agarwal, Shilpa; van Es, Daan; Heeres, Hero Jan

Published in:
Journal of Analytical and Applied Pyrolysis

DOI:
10.1016/j.jaap.2016.12.014

Publication date:
2017

Journal of Analytical and Applied Pyrolysis 123 (2017) 134–143

Contents lists available at ScienceDirect

Journal of Analytical and Applied Pyrolysis

journal homepage: www.elsevier.com/locate/jaap

Catalytic pyrolysis of recalcitrant, insoluble humin byproducts from C6 sugar biorefineries

Shilpa Agarwal [a], Daan van Es [b], Hero Jan Heeres [a,*]

[a] Chemical Engineering Department, ENTEG, University of Groningen, Nijenborgh 4, 9747 AG Groningen, The Netherlands
[b] Food & Bio-based Research, Wageningen University and Research Centre, 6700 AA Wageningen, The Netherlands

ARTICLE INFO

Article history:
Received 13 August 2016
Received in revised form
13 December 2016
Accepted 17 December 2016
Available online 21 December 2016

Keywords:
Pyrolysis
Humins
Catalyst
HZSM-5
Aromatics
Biobased chemicals

ABSTRACT

Humins are solid by-products formed during the acid-catalysed conversions of C-6 sugars to platform chemicals like hydroxymethylfurfural and levulinic acid. We here report an experimental study on the liquefaction/depolymerisation of humins using catalytic pyrolysis. Synthetic humins (SH) and crude industrial humins (CIH, including purified industrial (PIH) samples) from the acid-catalysed conversion of C-6 sugars to HMF/LA were tested. Thermal degradation patterns of both humin types vary significantly. Major thermal decomposition of the industrial humins was observed between 50 and 650 °C (weight loss approx. 66 wt%), whereas, major weight loss was observed between 200 and 800 °C for the synthetic humins (47 wt%). A series of catalytic pyrolysis tests with synthetic humins and different zeolites were performed using a PTV-GC/MS (humin to catalyst wt ratio of 0.2, 550 °C). Best results were obtained using HZSM-5 (SiO_2/Al_2O_3 = 50). For quantitative analysis, a gram scale pyrolysis unit was used, giving a product oil (9–11 wt% on humin intake) with approximately 1.5 and 10 wt% aromatics from synthetic and crude industrial humins, respectively. GPC data on the product oils clearly shows the breakdown of the humin structure into low molecular weight species. The HHV value of the liquid products (up to 41 MJ kg^{-1}) is considerably higher than that of the crude industrial humin feed (21–24 MJ kg^{-1}).

1. Introduction

Due to the availability and vast abundance, lignocellulosic biomass is considered as a potential feedstock for renewable fuels and valuable bulk chemical products [1,2]. In the last decade substantial efforts have been made to develop economically viable valorisation routes to convert biomass to valuable products [1,3–6].

Cellulose and hemicellulose form a major part of lignocellulosic biomass (70–80 wt%). One of the pathways investigated to date is the conversion of the cellulose and hemicellulose fraction into bio-based platform chemicals like 5- hydroxymethylfurfural (HMF) and levulinic acid (LA) [7,8] . HMF is considered a versatile chemical building block for C-6 compounds, such as alkoxymethylfuranics, 2,5-furandicarboxylic acid, 2,5-dimethylfuran, adipic acid, 1,6-hexanediol and caprolactam [8–10]. The demand for HMF as a platform chemical has already lead to the opening of a pilot plant by the Dutch company Avantium with the aim to produce 40 tonnes/year of HMF, which may subsequently be used to make PEF (polyethylene furanoate), a bio-based, recyclable polymer that can be used as a substitute for PET [11,12]. Furthermore, LA has also been identified as an important platform chemical for the production of fuel additives, monomers for plastics and textiles, and chemicals [13,14].

Both HMF and LA can be obtained by the dehydration of C-6 sugars using acid catalysts, but this inevitably leads to the formation of humin byproducts [15,16]. Depending on the process parameters, such as type of substrate, acid catalyst, temperature, and time, humin yields can vary from 5 to 50 wt% [7,17]. For instance in the Biofine process, a semi-commercial process to produce LA from lignocellulosic biomass, humin formation may be up to 20 wt% on feed, and its formation poses considerable challenges in terms of scale up (e.g. fouling, complex work-up) [18]. For HMF or LA production to become economically viable, there is need to either optimise the processes by suppressing the formation of humins, or, alternatively, to upgrade these humin byproducts into valuable chemicals.

In recent studies, it has been shown that humins are carbonaceous, heterogeneous, poly-disperse materials consisting of a furan-rich polymer network containing different functional groups [7,9,17,19]. Based on this knowledge, a few valorisation approaches

* Corresponding author.
E-mail address: h.j.heeres@rug.nl (H.J. Heeres).

http://dx.doi.org/10.1016/j.jaap.2016.12.014

have already been suggested in literature, including thermal and catalytic gasification as well as humin introduction in PFA (polyfurfuryl alcohol) to make an elaborate composite with enhanced properties [12,17].

In our previous work we have reported the thermal pyrolysis, a mature and commercially available technology [20–25], as a potential route to convert humins into a pyrolysis oil enriched with low molecular weight compounds [7] . The aim of this approach is to convert a solid, low energy density feed into an easily transportable fuel with a high energy density. The pyrolysis oil can potentially be used as a co-feed in power stations, as a boiler fuel, or to isolate high added value bulk chemicals, such as acetic acid and formic acid. Catalytic versions of pyrolysis technology have been developed recently for a range of lignocellulosic biomass sources and are considered an interesting route to obtain low molecular weight aromatics like benzene, toluene, and xylene (BTX) [26–29]. We here report a study on the catalytic pyrolysis of humins. Our aim is to obtain liquefied products with a high carbon efficiency and which are potentially enriched in valuable bulk chemicals like BTXNE (benzene, toluene, xylenes, naphthalene, ethylbenzene). Catalytic pyrolysis has to the best of our knowledge not been used for humin valorisation. This route is motivated by the fact that it has been shown that furanics, which are considered the main building blocks of humins, can be successfully converted to aromatics in the presence of a zeolite catalyst [30]. In this work, we have used two types of humins: synthetic humins (SH) obtained by treatment of D-glucose in aqueous media with a strong mineral acids, and crude industrial humins (CIH) obtained from Avantium Chemicals, the byproduct of the conversion of C-6 sugars to HMF in methanol as the solvent. In addition a purified form of the Avantium humins (PIH) was also tested.

2. Materials and methods

2.1. Chemicals

D-Glucose (99%) and sulphuric acid (95–97%) used for synthesis of synthetic humins were purchased from Sigma Aldrich and Merck KGaA, respectively. Tetrahydrofuran (THF) was used as a solvent and was obtained from Boom B.V. All the zeolite catalysts (Ferrierite 20, HY 5.1, NaY 5.1, HY 80, Mordenite 20, Na-Mordenite 13, Beta-25, HZSM-5 (SiO_2/Al_2O_3 = 23, 50, 80)) used in this study were purchased from Zeolyst. Relevant properties of the catalysts are provided in Tables S1 and S2 (Supplementary information). The hydrotalcite catalyst was obtained from Sigma Aldrich.

2.2. Industrial humins

Crude industrial (from Avantium) humins (CIH) were obtained as the waste stream from the catalytic dehydration of a carbohydrate feedstock in methanol to produce, methoxymethyl furfural (MMF) and methyl levulinate. This process is operated by Avantium Chemicals at their pilot plant facilites in Geleen, The Netherlands. The industrial humins were further purified using solvent extractions to remove the residual monomers (MMF, levulinic acid). Details of the extraction procedure and characterisation of the purified industrial humins (PIH) are given in reference [31].

2.3. Preparation of synthetic humin samples

The synthetic humins (SH) used in this study were synthesised by the acid catalysed hydrothermal reaction of D-glucose (1 M) using 0.01 M H_2SO_4 [7,19]. The clear solution of the sugar and acid was transferred to a stainless steel autoclave (1 L) equipped with an overhead stirrer and flushed with N_2 before heating. The solution was subjected to a hydrothermal treatment at 180 °C (heating rate: 1.3 °C/min; stirring rate: 120 rpm) for 8 h. The maximum pressure in the autoclave at 180 °C was 15–18 bar. After the hydrothermal treatment, the precipitates were separated using vacuum filtration, the residue was washed with 3 L deionised water and then vacuum dried at 60 °C overnight. Dried synthetic humins were ground and purified using a Soxhlet extraction with water for 24 h. Finally, the purified humins were vacuum dried for 24 h at 60 °C and ground into a powder.

2.4. Analytical methods

Elemental analyses (C, H, N, O, and S content) of the humins and residue after catalytic pyrolysis were carried out using an automated Euro Vector EA3000 CHNS analyser with acetanilide as the calibration reference. The oxygen content was determined by the difference of CHNS. All samples were analysed at least in duplicate and the average values are reported.

Thermogravimetric analysis (TGA) of all the humin samples was performed using a Mettler–Toledo analyser (TGA/SDTA851e). The humin samples were heated from 30 to 900 °C in nitrogen atmosphere, with a heating rate of 10 °C/min.

BET surface areas of the zeolites were determined by performing N_2 physisorption experiments using a Micromeritics Tristar instrument. The samples were degassed in vacuum at 300 °C for 24 h prior to the analysis.

Temperature programmed desorption of ammonia (NH_3-TPD): NH_3-TPD measurements were performed using a Micrometrics AutoChem II 2920 system (Micromeritics, Norcross, GA, USA). Before a TPD experiment, the catalyst (~60 mg) was degassed at 600 °C at a heating rate of 10 °C/min in a He flow for 60 min. Then the sample was cooled to 100 °C under a He flow. In the next step, the sample was saturated with a gas containing 1% of NH_3 in He flow at 100 °C for 60 min. Then, the sample was purged with a He flow at 100 °C until a constant baseline level was attained. The TPD measurement was performed in the temperature range 100–600 °C at a rate of 10 °C/min using He as the carrier gas. The evolved NH_3 was detected by an on-line thermal-conductivity detector, calibrated by the peak area of known pulses of NH_3.

2.5. Catalytic pyrolysis experiments

2.5.1. Small-scale (catalytic) pyrolysis

Small-scale (mg-scale) pyrolysis of humins was performed using a PTV injector (programmable temperature vaporiser, Model: Optic 2 from Atlas) placed on a HP 5890 GC Series II system in combination with a HP 5972 MS detector (PTV-GC/MS) controlled by an Optic 2 device (Fig. 1). For catalytic experiments, the humin was first loaded in the sample vial followed by the catalyst. Typically, for thermal pyrolysis, 0.5 mg of humin sample was used, whereas for catalytic pyrolysis, a humin to catalyst weight ratio of 0.2 was used in most experiments (catalyst screening using synthetic humins). However, for catalytic pyrolysis experiments comparing different humin types, a humin to catalyst weight ratio of 0.05 was used due to geometrical constraints of the sample vial. It must be noted that no significant difference in product yields were observed when the humin to catalyst ratio was changed from 0.2 to 0.05 (see Fig. S1 in Supplementary information).

Based on the preliminary pyrolysis tests, we observed maximum volatile yields at 550 °C (results not shown) and hence 550 °C was used as the pyrolysis temperature in this study. The pyrolysis temperature programme was set to ramp from 40 °C to 550 °C at a rate of 16 °C/s followed by an isothermal period at 550 °C for 60 s. After (catalytic) pyrolysis in the injector, the products were transferred to a capillary column (Agilent Technologies VF–5 ms, 30 × 0.25 × 1.0, split 50:1). Helium was used as the carrier gas at a flow rate of 1 mL/min. For GC measurements the following temperature profile

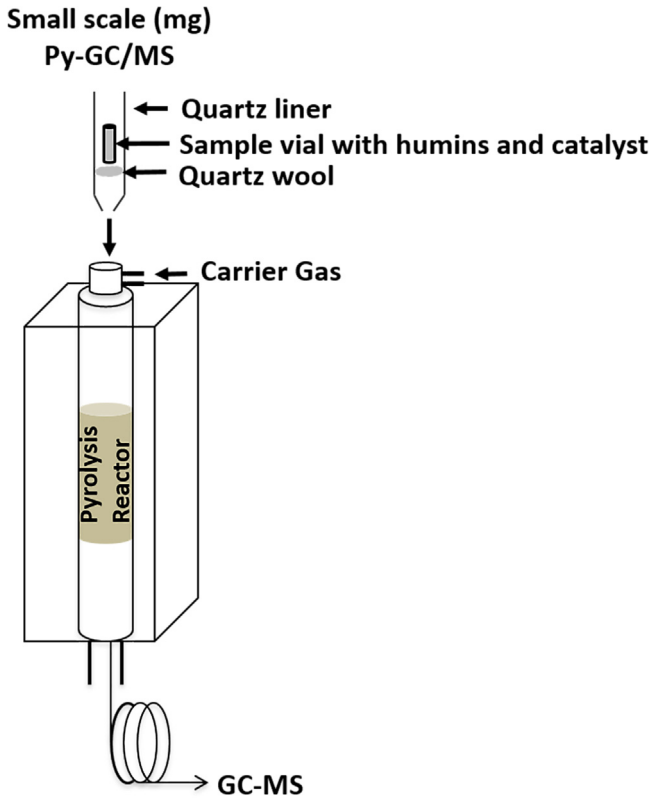

Fig. 1. Pyrolysis GC–MS (small scale) setup.

was used: initial temperature of 40 °C for 60 s followed by heating with a rate of 10 °C/min to the final temperature of 250 °C. The MS detector was operated in the scan range of m/z 35–400 using the electron ionisation mode (70 eV) with an interface temperature of 280 °C. Pyrolysis products were identified using the NIST05a mass spectra library.

In order to get a semi-quantitative estimate of the concentration of GC/MS detected compounds, the total ion chromatogram (TIC) peak areas of the MS detector were used as an approximation. It was assumed that the TIC peak area percentage of a certain compound is linearly correlated to the concentration of the corresponding compound. Therefore, to calulate the semi-quantitative yields of each compound/group of compounds, the corresponding TIC peak area percentage was divided by the TIC peak area of all the GC detectables. This methodolgy has often been reported for analysing the composition of biomass-derived pyrolysis product stream. For simplicity, the compounds, except BTXE, were classified based on chemical functionalities, e.g., aromatic derivatives (substituted benzene and polycyclic aromatics), furans and derivatives, napthalenes (napthalene and subsituted napthalenes), phenolic derivatives (substituted), and others (mainly alkanes, alkenes, acetic acid, indanes etc).

To determine the yields of BTXNE using PTV-GC/MS, an external standard solution with known quantities of BTXNE, was used to calculate the response factor. It was assumed that the concentration of the compounds is lineraly proportional to the total ion chromatogram peak area. A measurement using an external standard solution was performed prior to each set of experiments.

2.5.2. Gram-scale (catalytic) pyrolysis

Gram-scale pyrolysis was performed using an in house built reactor setup consisting of two stainless steel reactors (one reactor for the humins and one for the catalyst, Fig. 2). The pyrolysis products from the pyrolysis reactor pass through the catalyst bed for catalytic upgrading of the vapour stream. Immediately after the catalytic reactor, the condensable vapours were collected in two consecutive condensors immersed in isopropanol/liquid nitrogen mixtures maintained at −50 °C. Non-condensable vapour phase products were collected in a gas bag (SKC Tedlar 0.5 L sample bag). Nitrogen (Linde 3.0, 11 mL/min) was used as a carrier gas. For heating, the whole reactor system was immersed in a fluidised sand bath maintained at 570 °C. The duration of the pyrolysis reaction was 10 min. Mass balance calculations were performed by determination of the weight difference of the reactors, coolers and their connections before and after pyrolysis. The amount of non condensables (gas phase) was calculated by weighing the amount of water displaced when the gas bag was carefully submerged in a beaker filled with water. The liquid products were collected from the coolers and reactor tubes by rinsing with THF. As the water and oil are both miscible in THF, a single phase product liquid was obtained.

The water content in the pyrolytic humin oils obtained after gram-scale pyrolysis was determined by Karl Fischer titrations using a Metrohm Titrino 758 titration device. A small amount of sample (approximately 0.02–0.06 g) was added to an isolated glass chamber containing Hydranal® (KarlFischer Solvent, Riedel de Haen). The titrations were carried out using the Karl Fischer titrant Composit 5 K (Riedel de Haen). The water content of the THF was also measured and subtracted from the final value of the pyrolytic humin oil. All measurements were performed in duplicate and the average value is reported. The amount of the organic phase was calculated by subtracting the water content of the product from the total product liquid obtained after reaction.

For quantification of liquid phase components, the humin oils obtained after gram-scale experiments were analysed using GC/MS-FID. GC/MS spectra were recorded using a Quadrupole Hewlett-Packard 6890 MSD connected to a Hewlett-Packard 5890 gas chromatograph (GC) with a Restek RTX-1701 column (60 m × 0.25 mm i.d. and 0.25 μm film thickness) and flame ionisation detector (FID). Injection and detection were performed at 280 °C, using oven temperature heating profiles from 40 to 250 °C at a rate of 3 °C/min. Peak identification was done using the NIST05a mass spectra library. Quantification of products in pyrolytic humin oil was determined by using average relative response factor (RRF) of each component calculated with respect to *n*-nonane (internal standard).

Gas phases were collected during catalytic pyrolysis in a gasbag (SKC Tedlar 0.5 L sample bag (6″ × 6″)) with a polypropylene septum fitting. Quantification of the main gas phase components was done uisng GC-TCD analyses. These were performed on a Hewlett Packard 5890 Series II GC equipped with a Poraplot Q Al_2O_3/Na_2SO_4 column and a molecular sieve (5 Å) column. The injector temperature was set at 150 °C and the detector temperature was maintained at 90 °C. The oven temperature was kept at 40 °C for 2 min then heated up to 90 °C at the rate of 20 °C/min and kept at this temperature for 2 min. A reference gas was used to identify the peaks by retention time and to quantify the products in the gas phase (55.19% H_2, 19.70% CH_4, 3.00% CO, 18.10% CO_2, 0.51% ethylene, 1.49% ethane, 0.51% propylene and 1.50% propane).

GPC analyses were performed on the humin oils using an HP1100 equipped with three 300 × 7.5 mm PLgel 3 μm MIXED-E columns (temperature maintained at 42 °C during measurements) in series using a GBC LC 1240 RI detector. Average molecular weight calculations were performed with the PSS WinGPC Unity software from Polymer Standards Service. Polystyrene samples were used as the calibration standard. For GPC measurements, THF was used as eluent at a flow rate of 1 mL/min at 140 bar, with an injection volume of 20 μL. All the samples before GPC analysis were filtered using 0.2 μm PTFE filter to trap particles, if any, that may affect the analysis.

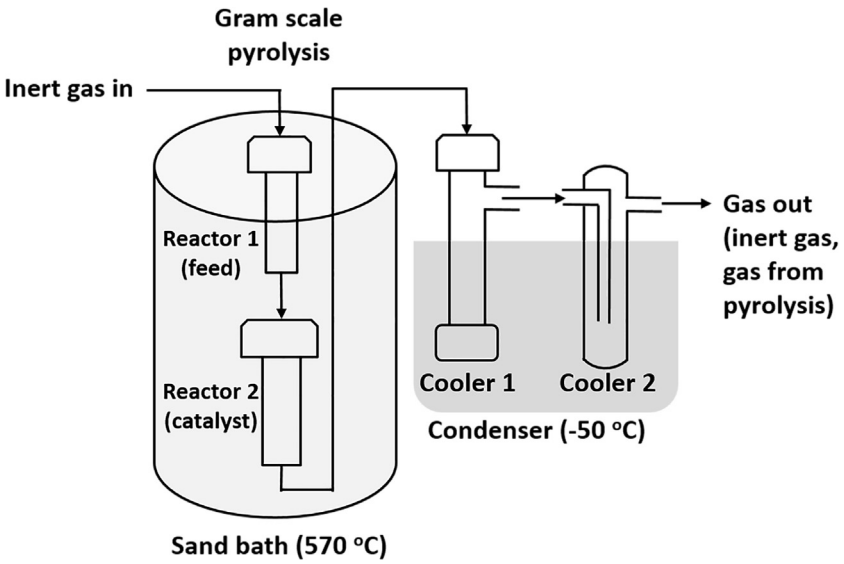

Fig. 2. Pyrolysis gram scale setup.

3. Results and discussion

3.1. Characterisation of the humin samples

3.1.1. Elemental composition of the humins

The synthetic humin contains approximately 66 wt% [C], 30 wt% [O] and 4 wt% [H], see Table 1 for details. These values agree well with the reported values in the literature [7,19]. The elemental composition of the synthetic humins is significantly different from than that of the starting material (D-glucose) due to dehydration/condensation reactions involving sugar molecules and intermediates [7,8].

For the industrial humins, the carbon content is lower than for the synthetic humin, whereas the hydrogen and oxygen contents are higher. The H/C and O/C ratios of industrial humins were observed to be similar to those for HMF, see Table 1. These observations indicate that the industrial humin samples are less dehydrated than the synthetic humins.

3.1.2. Thermogravimetric behaviour of the humin samples

To gain more insight into the thermal behaviour of the humin samples, thermogravemetric analyses were performed in an inert (N_2) atmosphere. The change in the weight of the humin samples as a function of temperature is shown in Fig. 3. It is clearly evident that the thermal behaviour of the synthetic and industrial (including purified) humin samples are very different. Initial weight losses starts around 50 °C for the industrial humin samples and levels off at around 650 °C (weight loss was approximately 66 wt%). For the purified industrial humins (PIH) the thermal decomposition pattern is quite similar to the crude sample, however the total weight loss is about 57 wt%. This decrease in weight loss compared to the crude sample indicates that low molecular weight compounds are present in the crude industrial humin sample. For synthetic humins, the major weight loss was observed between 200 and 800 °C (about 47 wt%). These observations indicate that the gas and liquid yields for industrial humins (including PIH) during pyrolysis are expected to be higher than synthetic humins.

As can be seen in Fig. 3 (right plot), the highest degradation rate for the synthetic humins was observed at 430 °C whereas for industrial humins sharp peaks were seen at 180 and 200 °C. The presence of this sharp degradation peak in case of industrial humins points towards the presence of considerable amounts of volatile, low molecular weight components. After purification of the industrial humins, the sharp peak at 180 °C disappears and this points towards the partial removal of (trapped) low molecular weight compounds.

Table 1
Elemental composition of the humin samples and relevant model compounds.

Humins	C (wt%)	H (wt%)	O (wt%)	H/C	O/C
Synthetic	65.7	4.4	29.9	0.80	0.34
Crude industrial	56.7	5.4	37.9	1.12	0.50
HMF	57.1	4.8	38.1	1.0	0.50
Levulinic acid	51.7	6.9	41.3	1.6	0.6
Glucose	40	6.7	53.3	2.0	1.0

3.2. Thermal pyrolysis of humins

Thermal, non-catalytic pyrolysis was performed on represenative samples at 550 °C using PTV-GC/MS (mg-scale) to obtain insight in the composition of the vapour phase. The chromatograms for all the humin samples are shown in Fig. 4. Mainly furanics, such as 2-methylfuran, 2,5- dimethylfuran, 1,2-furanylethanone were observed in the case of synthetic humins, confirming that synthetic humins contain a considerable amount of furanic moieties [7,19]. Interestingly, for the industrial humins and PIH, in addition to the furanics, monomeric species like HMF, levulinic acid and their methyl esters were also observed. This observation indicates that industrial humins not only consist of condensed furanics rings but also contain trapped monomeric intermediate/products. This is in agreement with the elemental analysis (Table 1) and TGA (Fig. 3) data. Furthermore, after purification of the industrial humins, these monomers were still present in the vapour phase, which indicates that some of these monomers are actually incorporated in the core structure of the humins.

3.3. Catalytic pyrolysis of humins

3.3.1. Catalytic pyrolysis using synthetic humins

A series of pyrolysis tests with synthetic humins and different zeolites were performed in the PTV-GC/MS (humin to catalyst wt ratio of 0.2) at 550 °C to identify the best catalyst to obtain liquefied products with a high carbon efficiency and potentially enriched in valuable bulk chemicals like BTXNE.

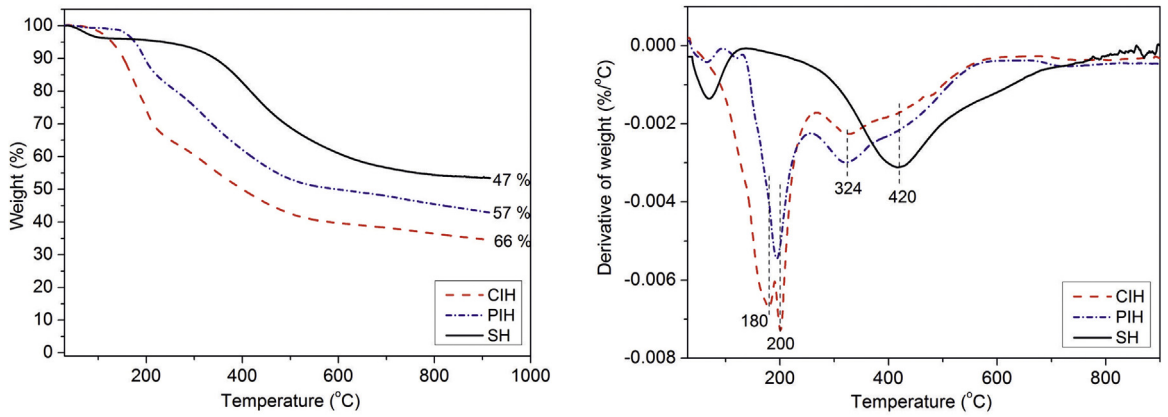

Fig. 3. TGA (left) and DTG (right) plots of crude industrial (CIH, red dash line), purified industrial (PIH, blue dash-dot) and synthetic (SH, black solid line) humins. (For interpretation of the references to color in this figure legend, the reader is referred to the web version of this article.)

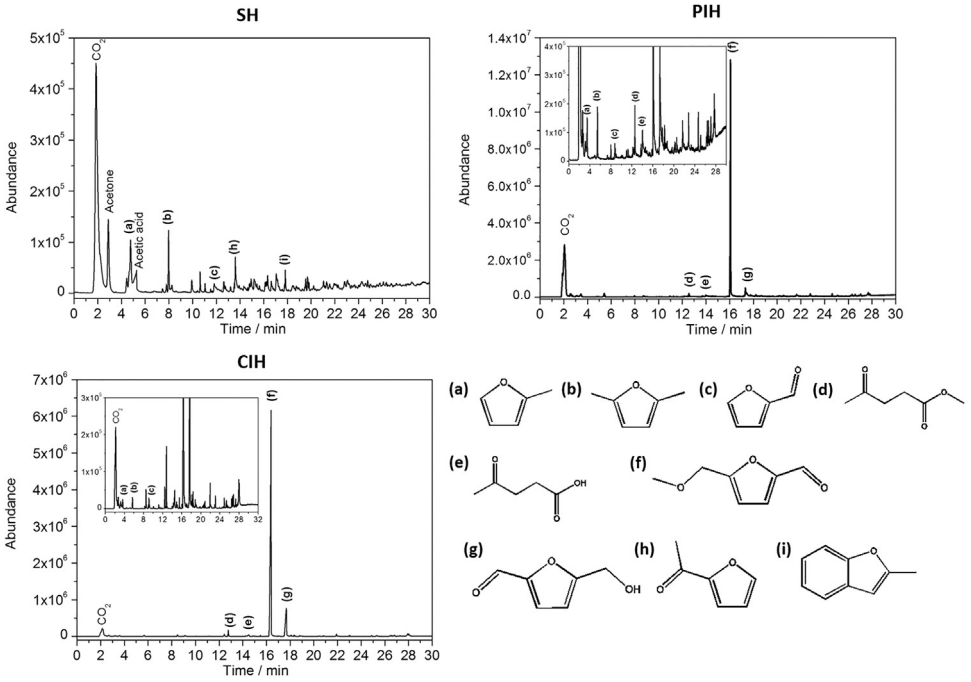

Fig. 4. Pyrolysis GC/MS chromatogram of SH, PIH and CIH at 550 °C.

As mentioned earlier, furanics were predominantly observed after pyrolysis of synthetic humins at 550 °C in the absence of catalyst, and no trace of aromatics was observed (Fig. 4). However, on pyrolysis at 550 °C in the presence of a catalyst, the product distribution significantly changed, as can be seen in Fig. 5 and considerable amounts of BTXNE are formed, the exact amount being a function of the zeolite used.

We believe that the humins first depolymerize thermally as well as catalytically on the outside surface of the zeolites. These depolymerized fragments react further at the surface and inside the pores to give aromatic products. A similar mechanism has been reported for the catalytic cracking of polymers like low density polyethylene on zeolites [37]. The aromatics are most likely formed by Diels-Alder addition reactions between furanics and olefines (Scheme 1). In a model compound study [30,38], it has already been demonstrated that aromatics are formed by co-feeding olefins and furanics over for instance a HZSM-5 catalyst.

Remarkable differences in aromatics (BTXNE) yields were observed for the various catalysts. Lowest BTXNE yields were found for NaY, Na-mordenite and the basic hydrotalcite catalyst (Fig. 5). These findings reveal that acidic, protonated zeolites are desirable for the aromatization of the pyrolytic vapours [32–35]. For the acidic zeolites, the BTXNE yields increase in the order: Ferrierite 20 < HY–80 < HY 5.1 < H-Mordenite 20 < H- ZSM-5 (Fig. 5). These differences are expected to be related to zeolite properties like pore dimensions and average pore size (Table S1), BET surface area and acidity (Table S2).

In this respect, the poor performance of Ferrierite 20 may be due to the small pore dimensions and the pore size of this zeolite (Table S1). This is agreement with literature data, where the low aromatic yield for this zeolite is associated with diffusion limitations in the catalyst pore system due to the small pore sizes [32].

A clear relation between the BET surface area of the catalysts (Table S2) and the BTXNE yield is absent, though the highest yields were obtained with zeolites with high BET surface areas. Upon suggestion of one of the reviewers, a catalytic pyrolysis experiment has been performed with Beta-25 zeolite in the mg scale set-up. The

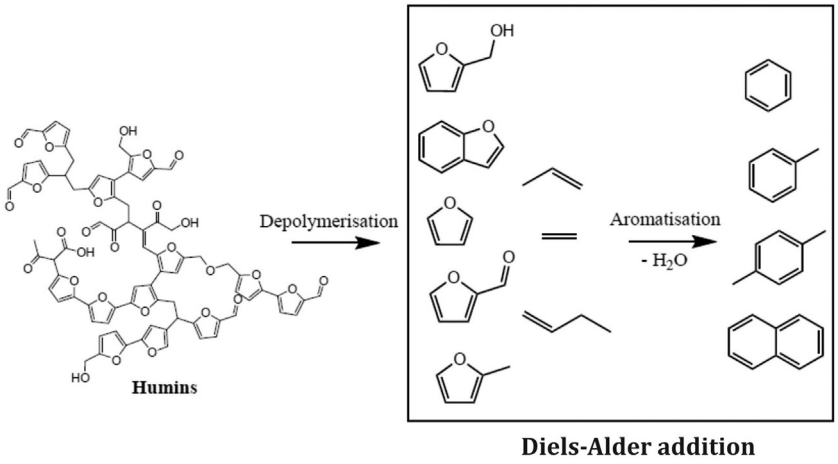

Scheme 1. Proposed reaction pathway for the catalytic pyrolysis of humins.

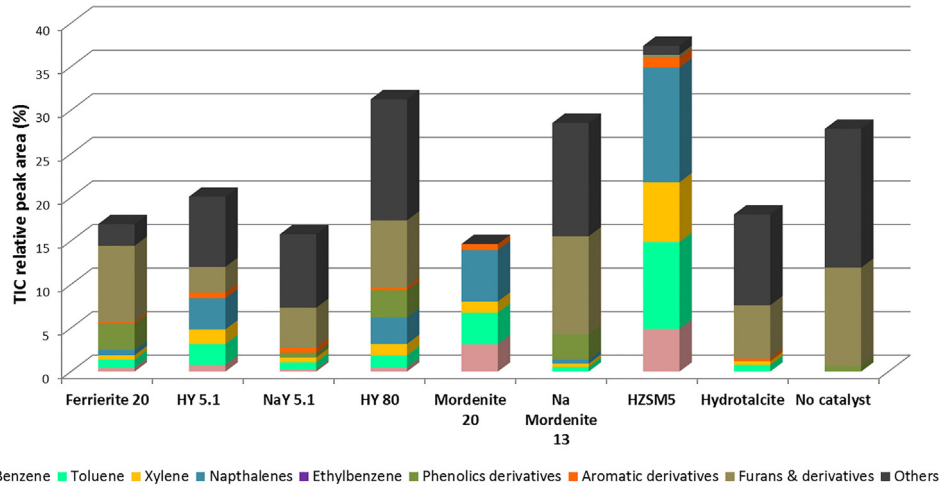

Fig. 5. Representative GC detectable monomeric volatiles released during the catalytic pyrolysis of synthetic humins (SH) with different zeolite catalysts (Humin to catalyst wt. ratio of 0.2) at 550 °C.

BTXNE yield was about half of that observed for H-ZSM-5 (Fig. S2, Supplementary information).

The good performance of the H-ZSM-5 catalysts is likely related to its acidity in combination with the pore structure/sizes. Studies in the literature have already shown that HZSM-5 has the optimal zeolite pore structure to obtain the highest yields of aromatics from the catalytic pyrolysis of biomass [36]. As such, it appears that HZSM-5 has the optimum geometry for furanics, the primary thermal products from humin pyrolysis, to enter the pores and to be converted into aromatics.

3.3.2. Catalytic pyrolysis of synthetic and industrial humins using HZSM-5

As HZSM-5 was shown to be the most promising catalyst for the synthetic humins, the next step in this study was to investigate the effect of the acidity of HZSM-5 during the catalytic pyrolysis of both industrial and synthetic humins. We performed the catalytic pyrolysis tests using HZSM-5 with different SiO_2/Al_2O_3 ratios (23, 50 and 80) and as such with different acidity (highest for 23). It is apparent from Fig. 6 that HZSM-5 with a SiO_2/Al_2O_3 ratio of 50 gives the highest yield of aromatics for both types of humins. With a further increase in the acidity (from 50 to 23) a decrease in the aromatic yield was observed. It is evident that higher Brönsted acidity is desirable for aromatic yields, however a too high value leads to lower yields.

To estimate the yields of aromatics on humin intake, an external standard solution with known BTXNE concentrations was used. Based on the small-scale pyrolysis (Py-GC/MS) experiments (Fig. 7), the BTXNE yield is significantly higher for industrial humins (10 wt%) in comparison to the synthetic one (1.5 wt%). As expected for PIH samples, the BTXNE yields (5 wt%) are intermediate between the crude industrial and synthetic humins. We further determined the BTXNE yield for kraft lignin under similar pyrolysis conditions with the incentive to compare the yields for humins and lignin, the latter being considered a promising source for BTXNE. With kraft lignin, a BTXNE yield of 6 wt% (on lignin intake) was obtained by catalytic pyrolysis. The higher BTXNE values for industrial humins clearly indicate that industrial humins have potential to be used as feeds for the production of bio-based aromatics.

During catalytic pyrolysis, the color of the HZSM-5-50 catalyst changed from off white/grey to black, an indication for coke formation, which is well established for catalytic pyrolysis of lignocellulosic biomass. To check whether coke removal is possible and does not lead to irreversible deactivation, the spent catalyst was calcined at 550 °C in air for 4 h. No difference in the catalytic activity was observed when using the regenerated catalyst, as was evident from the amounts of low molecular weight products formed. Further work is suggested to investigate the long term stability of the catalyst after repeated catalytic-oxidative work-up cycles.

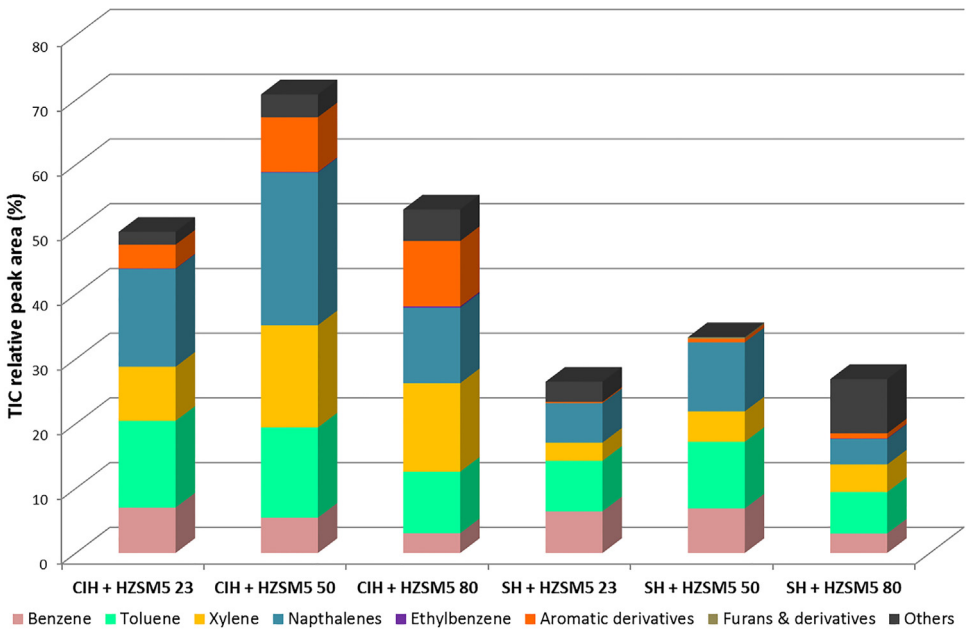

Fig. 6. Effect of the SiO_2/Al_2O_3 ratio of the HZSM-5 zeolite on the product distribution for the catalytic pyrolysis of crude industrial (CIH) and synthetic (SH) humins (Humin to catalyst weight ratio of 0.05) at 550 °C.

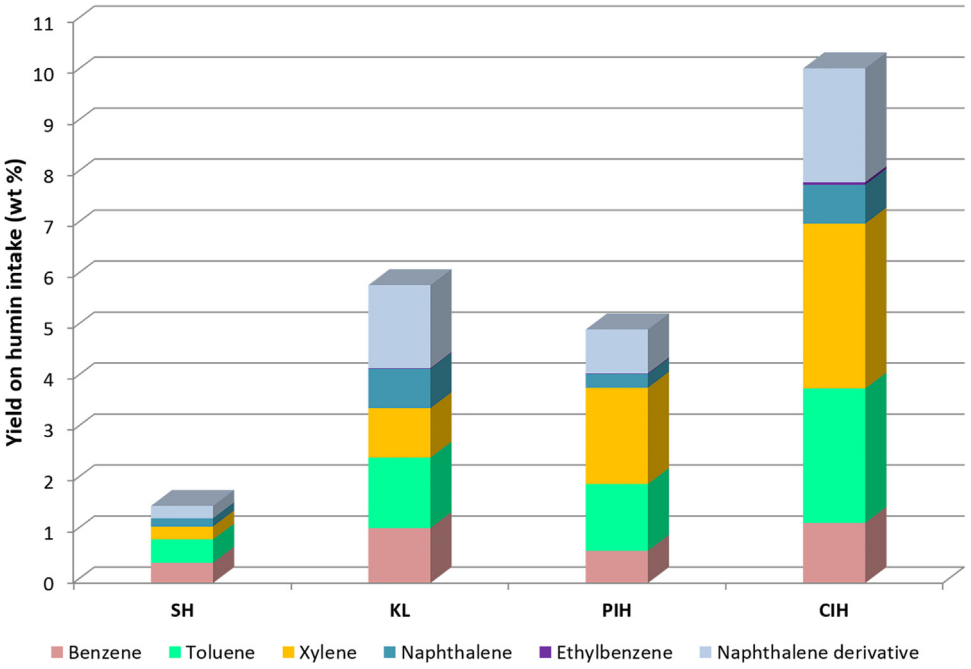

Fig. 7. BTXNE yields on humin intake obtained during the pyrolysis of synthetic (SH), crude/purified industrial (CIH/PIH) humins and kraft lignin (KL) with HZSM-5-50 (Humin: Catalyst weight ratio = 1:20) at 550 °C.

3.4. Gram-scale pyrolysis

In addition to the small scale catalytic pyrolysis experiments, catalytic pyrolysis experiments were performed with industrial and synthetic humins at gram-scale to obtain humin oils for detailed product analysis and to estimate the mass balance closures. It must be noted that THF was used to collect the products from the reactor tubes and coolers and this hampers the accuracy of the oil yield determinations.

Based on mass-balance calculations (Fig. 8), an oil yield of approx. 11–14 wt% was obtained for the catalytic pyrolysis of both industrial and synthetic humins. The solid residue for the synthetic humins (58 wt%) after reaction is much higher than for the industrial ones (38 wt% on humin intake), in agreement with the TGA data (Fig. 3).

The oil phase was further characterised using GC/MS-FID to gain detailed insights into product yields and composition (Table 2). The total amount of detectable aromatic species for industrial and synthetic humins were at max. 9 and 2 wt% on humin intake, respectively, which confirms the results from the PTV-GC/MS experiments. As a large fraction of the humin oils (especially in the case of synthetic humins) was not observed by GC and is likely non-volatile and of higher molecular weight, we further analysed the product oils using GPC (Fig. 9). The GPC spectra do not clearly show

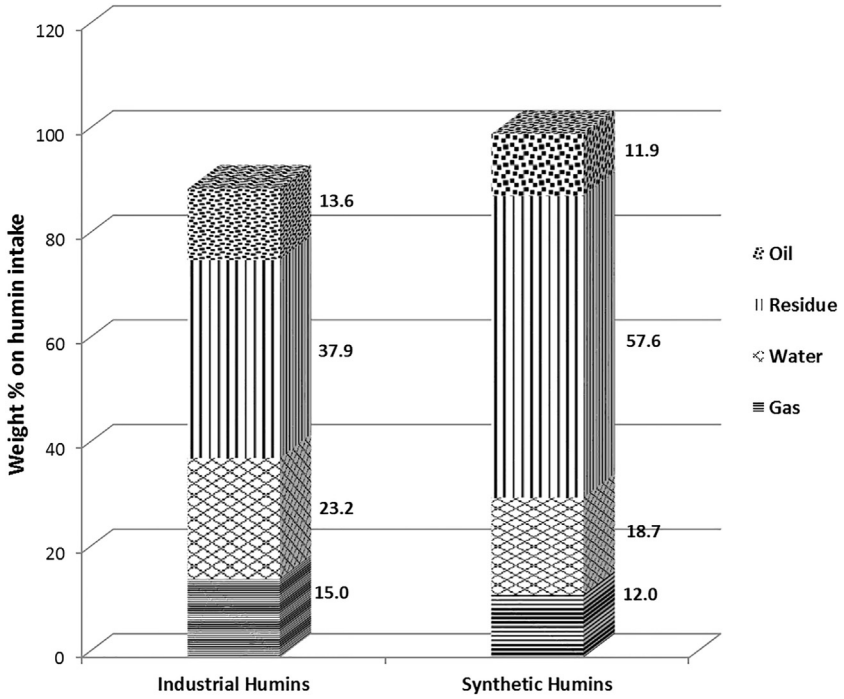

Fig. 8. Product distribution for the catalytic pyrolysis of crude industrial (CIH) and synthetic humins (SH) with HZSM-5-50 at 550 °C (Humin to catalyst weight ratio of 0.2) in the g-scale reactor.

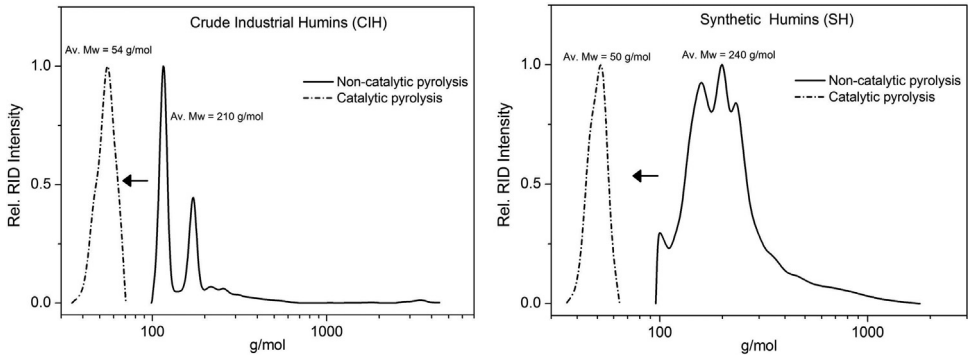

Fig. 9. Gel permeation chromatograms (GPC) of humin oils obtained after non-catalytic and catalytic (with HZSM-5-50) pyrolysis of crude industrial (left) and synthetic (right) humins at 550 °C. Molecular weight values are relative numbers based on polystyrene standards.

Table 2
Distribution of pyrolysis products (wt% on humin intake) for the catalytic pyrolysis of various humins samples using gram scale pyrolysis.

Compound class	Crude Ind. humins (CIH)	Synthetic humins (SH)
Aromatics	5.64	1.35
Napthalenes	2.00	0.70
Indane/Indenes	0.80	0.01
Alkanes	0.09	0.01
Polyaromatics	0.26	0.11
Total	8.79	2.18

the presence of higher molecular weight species in the product oils, though some tailing, associated with higher molecular weight compounds, cannot be excluded. As such, the differences in oil yield based on mass balance calculations and the GC yields for BTXNE are likely due to the complex work-up of the oil phase (using THF) after pyrolysis which is prone to some experimental error.

A comparison between the GPC data for the catalytic and non-catalytic pyrolysis clearly reveals that the presence of a catalysts leads to a reduction of the molecular weight of the product oils. As such, the catalysts not only catalyse deoxygenation reactions but also are able to break down and crack the polymeric structure of the humins.

Finally, the elemental compositions of humin feeds and the solid residues obtained after catalytic pyrolysis were determined and results are plotted in the form of a van Krevelen diagram (Fig. 10). Both humin feeds have significantly different H/C and O/C ratios, however after pyrolysis the composition of the residue from both humin sources is quite similar. In both cases, the oxygen and hydrogen contents decreases significantly upon pyrolysis.

In addition, the higher heating value (HHV) of the humins and pyrolytic humin oils was estimated using the Milne equation (Eq. (1), where C, H, O and S are carbon, hydrogen, oxygen and sulphur in weight percentages, respectively. The Milne equation semi-quantitatively predicts the HHV of fuels or fuel resources obtained from coal, biomass, pyrolysis oil and biodiesel using elemental compositions. For HHV calculation of the product oil, we calculated the HHV value using the elemental composition of the products identi-

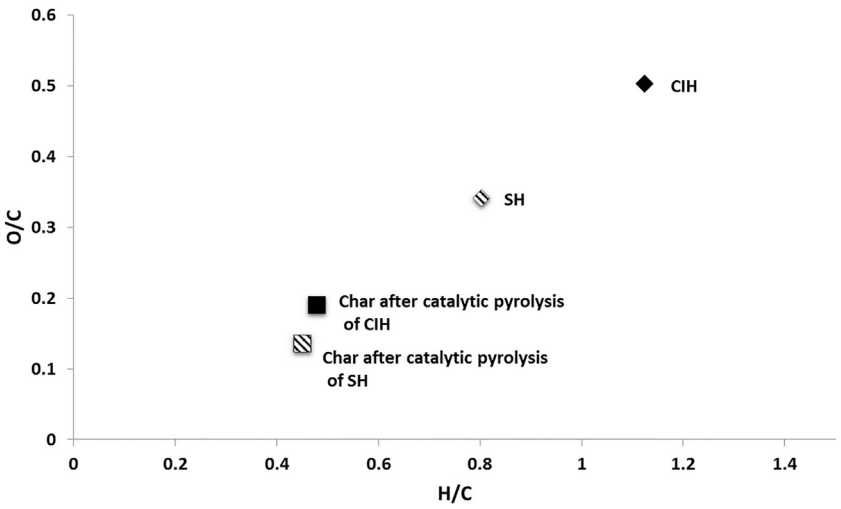

Fig. 10. van Krevelen diagram of the humin feeds and solid residues obtained after catalytic pyrolysis.

fied by GC–MS/FID (see Table S3 in supplementary information for details).

$$HHV_{Milne}\left(MJ.kg^{-1}\right) = 0.341 \times C + 1.322 \times H - 0.12 \times O - 0.12 \times N + 0.0686 \times S - 0.0153 \times residue \quad (1)$$

The HHV value the for industrial and synthetic humins was calculated to be 21 and 24 MJ kg^{-1}. After catalytic pyrolysis, the HHV value significantly increased to about 41 MJ kg^{-1} for the humin oils (industrial/synthetic). Moreover, the HHV of the char obtained after pyrolysis of humins was found to be about 30 MJ kg^{-1}, which is again higher than the starting feed value and can hence be potentially used as a co-feed in power stations or for combustion during pyrolysis. These results clearly provide the proof of principle that liquefaction of humins by catalytic pyrolysis to give a liquid product with a higher energy density is well possible, though the yield of humin oils (11–14 wt%) is low.

4. Conclusions

We have provided the proof of principle for the conversion of humins (industrial and synthetic ones) to humin oils (11–14 wt% on humin intake) enriched in valuable aromatics using catalytic pyrolysis. HZSM-5 (SiO_2/Al_2O_3 = 50) was found to be the most promising catalyst. Quantitative analysis of the humin oils shows the presence of approximately 2 and 10 wt% of aromatics based on synthetic and industrial humin intake, respectively. The HHV value of the humin oils was estimated to be about 41 MJ kg^{-1}.

The main components in the humin oils are high value low molecular weight aromatics. As such, the products have potential to be used as an additive for biofuels. In addition, isolated individual components may serve as building blocks for renewable polymers. Based on the stoichiometry of the reaction, the maximum theoritical yield of aromatics from the (catalytic) pyrolysis of humins is approximetely 50 wt% on humin intake. In this work we report an aromatic yield of 9 wt% for the industrial humin samples, which is about 18 wt% of the theoretical maximum.

Acknowledgements

This research was performed within the framework of the Catch-Bio program. The authors gratefully acknowledge the support of the Smart Mix Program of the Netherlands Ministry of Economic Affairs, Agriculture and Innovation and the Netherlands Ministry of Education, Culture and Science, project number 053.70.358. Authors acknowledge Avantium Chemicals BV, The Netherlands for providing industrial humins and Willem Vogelzang BSc. (WUR-FBR) for purifying the industrial humins. The authors are also grateful to Anne Appeldoorn, Erwin Wilbers and Marcel de Vries (University of Groningen) for technical support, Hans van de Velde (University of Groningen) for the elemental analysis, Leon Rohrbach (University of Groningen) for the NH_3-TPD measurement and K. Altena- Schildkamp for the BET measurements (CPM, University of Twente).

Appendix A. Supplementary data

Supplementary data associated with this article can be found, in the online version, at http://dx.doi.org/10.1016/j.jaap.2016.12.014.

References

[1] A. Corma, S. Iborra, A. Velty, Chemical routes for the transformation of biomass into chemicals, Chem. Rev. 107 (2007) 2411–2502.
[2] A.J. Ragauskas, C.K. Williams, B.H. Davison, G. Britovsek, J. Cairney, C.A. Eckert, W.J. Frederick, J.P. Hallett, D.J. Leak, C.L. Liotta, J.R. Mielenz, R. Murphy, R. Templer, T. Tschaplinski, The path forward for biofuels and biomaterials, Science 311 (2006) 484–489, 6185.
[3] D. Carpenter, T.L. Westover, S. Czernik, W. Jablonski, Biomass feedstocks for renewable fuel production: a review of the impacts of feedstock and pretreatment on the yield and product distribution of fast pyrolysis bio-oils and vapors, Green Chem. 16 (2014) 384–406.
[4] A.J. Ragauskas, G.T. Beckham, M.J. Biddy, R. Chandra, F. Chen, M.F. Davis, B.H. Davison, R.A. Dixon, P. Gilna, M. Keller, P. Langan, A.K. Naskar, J.N. Saddler, T.J. Tschaplinski, G.A. Tuskan, C.E. Wyman, Lignin valorization: improving lignin processing in the biorefinery, Science 344 (2014).
[5] C.O. Tuck, E. Pérez, I.T. Horváth, R.A. Sheldon, M. Poliakoff, Valorization of biomass: deriving more value from waste, Science 337 (2012) 695–699.
[6] G.W. Huber, S. Iborra, A. Corma, Synthesis of transportation fuels from biomass: chemistry catalysts, and engineering, Chem. Rev. 106 (2006) 4044–4098.
[7] C.B. Rasrendra, M. Windt, Y. Wang, S. Adisasmito, I.G.B.N. Makertihartha, E.R.H. van Eck, D. Meier, H.J. Heeres, Experimental studies on the pyrolysis of humins from the acid-catalysed dehydration of C6-sugars, J. Anal. Appl. Pyrol. 104 (2013) 299–307.
[8] R.-J. van Putten, J.C. van der Waal, E. de Jong, C.B. Rasrendra, H.J. Heeres, J.G. de Vries, Hydroxymethylfurfural a versatile platform chemical made from renewable resources, Chem. Rev. 113 (2013) 1499–1597.
[9] J. Horvat, B. Klaić, B. Metelko, V. Šunjić, Mechanism of levulinic acid formation, Tetrahedron Lett. 26 (1985) 2111–2114.
[10] T. Buntara, S. Noel, P.H. Phua, I. Melián- Cabrera, J.G. de Vries, H.J. Heeres, Caprolactam from renewable resources: catalytic conversion of 5-hydroxymethylfurfural into caprolactone, Angew. Chem. Int. Ed. 50 (2011) 7083–7087.
[11] A.J.J.E. Eerhart, W.J.J. Huijgen, R.J.H. Grisel, J.C. van der Waal, E. de Jong, A. de Sousa Dias, A.P.C. Faaij, M.K. Patel, Fuels and plastics from lignocellulosic

biomass via the furan pathway; a technical analysis, RSC Adv. 4 (2014) 3536–3549.
[12] J.-M. Pin, N. Guigo, A. Mija, L. Vincent, N. Sbirrazzuoli, J.C. van der Waal, E. de Jong, Valorization of biorefinery side-stream products: combination of humins with polyfurfuryl alcohol for composite elaboration, ACS Sustainable Chem. Eng. 2 (2014) 2182–2190.
[13] D.J. Braden, C.A. Henao, J. Heltzel, C.C. Maravelias, J.A. Dumesic, Production of liquid hydrocarbon fuels by catalytic conversion of biomass- derived levulinic acid, Green Chem. 13 (2011) 1755–1765.
[14] J.C. Serrano-Ruiz, D. Wang, J.A. Dumesic, Catalytic upgrading of levulinic acid to 5-nonanone, Green Chem. 12 (2010) 574–577.
[15] A.A. Rosatella, S.P. Simeonov, R.F.M. Frade, C.A.M. Afonso, 5-Hydroxymethylfurfural (HMF) as a building block platform: biological properties, synthesis and synthetic applications, Green Chem. 13 (2011) 754–793.
[16] K.M. Rapp, in, Google Patents (1988).
[17] T.M.C. Hoang, L. Lefferts, K. Seshan, Valorization of humin-based byproducts from biomass processing—a route to sustainable hydrogen, ChemSusChem 6 (2013) 1651–1658.
[18] D.J. Hayes, S. Fitzpatrick, M.H.B. Hayes, J.R.H. Ross, Biorefineries-Industrial Processes and Products, Wiley-VCH Verlag GmbH, 2008, pp. 139–164.
[19] I. van Zandvoort, Y. Wang, C.B. Rasrendra, E.R.H. van Eck, P.C.A. Bruijnincx, H.J. Heeres, B.M. Weckhuysen, Formation, molecular structure, and morphology of humins in biomass conversion: influence of feedstock and processing conditions, ChemSusChem 6 (2013) 1745–1758.
[20] A.V. Bridgwater, Renewable fuels and chemicals by thermal processing of biomass, Chem. Eng. J. 91 (2003) 87–102.
[21] A.V. Bridgwater, Review of fast pyrolysis of biomass and product upgrading, Biomass Bioenergy 38 (2012) 68–94.
[22] S. Chu, A.V. Subrahmanyam, G.W. Huber, The pyrolysis chemistry of a beta-O-4 type oligomeric lignin model compound, Green Chem. 15 (2013) 125–136.
[23] W. Mu, H. Ben, A. Ragauskas, Y. Deng, Lignin pyrolysis components and upgrading—technology review, BioEnergy Res. 6 (2013) 1183–1204.
[24] H. Yang, R. Yan, H. Chen, D.H. Lee, C. Zheng, Characteristics of hemicellulose cellulose and lignin pyrolysis, Fuel 86 (2007) 1781–1788.
[25] R. French, S. Czernik, Catalytic pyrolysis of biomass for biofuels production, Fuel Process. Technol. 91 (2010) 25–32.
[26] X. Li, L. Su, Y. Wang, Y. Yu, C. Wang, X. Li, Z. Wang, Catalytic fast pyrolysis of Kraft lignin with HZSM-5 zeolite for producing aromatic hydrocarbons, Front. Environ. Sci. Eng. 6 (2012) 295–303.
[27] D. Shen, J. Zhao, R. Xiao, S. Gu, Production of aromatic monomers from catalytic pyrolysis of black-liquor lignin, J. Anal. Appl. Pyrolysis 111 (2015) 47–54.
[28] M. Inaba, K. Murata, I. Takahara, Y. Liu, Catalytic fast pyrolysis of eucalyptus using zeolite, J. Chem. Eng. Jpn. 47 (2014) 345–351.
[29] M. Inaba, K. Murata, I. Takahara, Y. Liu, Production of aromatic and phenolic compounds by fast pyrolysis of eucalyptus using zeolite catalysts, J. Jpn. Inst. Energy 93 (2014) 944–952.
[30] Y.-T. Cheng, G.W. Huber, Production of targeted aromatics by using Diels-Alder classes of reactions with furans and olefins over ZSM-5, Green Chem. 14 (2012) 3114–3125.
[31] S. Constant, W. Vogelzang, R.K.P. Purushotaman, D.S. van Es, P.C.A. Bruijnincx, B.M. Weckhuysen, Characterisation of Soluble Industrial Humins, to be sumitted (2017).
[32] D.J. Mihalcik, C.A. Mullen, A.A. Boateng, Screening acidic zeolites for catalytic fast pyrolysis of biomass and its components, J. Anal. Appl. Pyrolysis 92 (2011) 224–232.
[33] N. Nikbin, S. Feng, S. Caratzoulas, D.G. Vlachos, p-Xylene formation by dehydrative aromatization of a Diels-Alder product in Lewis and Brønsted acidic zeolites, J. Phys. Chem. C 118 (2014) 24415–24424.
[34] D. Li, L. Wang, M. Koike, Y. Nakagawa, K. Tomishige, Steam reforming of tar from pyrolysis of biomass over Ni/Mg/Al catalysts prepared from hydrotalcite-like precursors, Appl. Catal. B 102 (2011) 528–538.
[35] T.R. Carlson, J. Jae, Y.-C. Lin, G.A. Tompsett, G.W. Huber, Catalytic fast pyrolysis of glucose with HZSM-5: the combined homogeneous and heterogeneous reactions, J. Catal. 270 (2010) 110–124.
[36] J. Jae, G.A. Tompsett, A.J. Foster, K.D. Hammond, S.M. Auerbach, R.F. Lobo, G.W. Huber, Investigation into the shape selectivity of zeolite catalysts for biomass conversion, J. Catal. 279 (2011) 257–268.
[37] A. Bonilla, D. Baudouin, J. Pérez- Ramírez, Desilication of ferrierite zeolite for porosity generation and improved effectiveness in polyethylene pyrolysis, J. Catal. 265 (2009) 170–180.
[38] Y.-T. Cheng, J. Jae, J. Shi, W. Fan, G.W. Huber, Production of renewable aromatic compounds by catalytic fast pyrolysis of lignocellulosic biomass with bifunctional Ga/ZSM-5 catalysts, Angew. Chem. Int. Ed. 51 (2012) 1387–1390.